

Condensates in Driven Aggregation Processes

E. Ben-Naim¹ and P. L. Krapivsky²

¹*Theoretical Division and Center for Nonlinear Studies,
Los Alamos National Laboratory, Los Alamos, New Mexico 87545*

²*Department of Physics and Center for Molecular Cybernetics,
Boston University, Boston, Massachusetts, 02215*

We investigate aggregation driven by mass injection. In this stochastic process, mass is added with constant rate r and clusters merge at a constant total rate 1, so that both the total number of clusters and the total mass steadily grow with time. Analytic results are presented for the three classic aggregation rates $K_{i,j}$ between clusters of size i and j . When $K_{i,j} = \text{const}$, the cluster size distribution decays exponentially. When $K_{i,j} \propto i + j$ or $K_{i,j} \propto i \times j$, there are two phases: (i) a condensate phase with a condensate containing a finite fraction of the mass in the system as well as finite clusters, and (ii) a cluster phase with finite clusters only. For $K_{i,j} \propto i + j$, the cluster size distribution, c_k , has a power-law tail, $c_k \sim k^{-\gamma}$ in either phase. The exponent is a non-monotonic function of the injection rate: $\gamma = r/(r - 1)$ in the condensate phase, $r < 2$, and $\gamma = r$ in the cluster phase, $r > 2$.

PACS numbers: 05.40.-a, 05.20.Dd, 89.75.Hc, 02.50.Ey

I. INTRODUCTION

Aggregation processes in which small objects merge irreversibly to form larger clusters are ubiquitous in nature [1, 2]. For example, aggregation underlies the evolution of planetary systems in astrophysics [3], cloud formation and dust accumulation in atmospheric sciences [4–7], as well as polymer and gel formation in chemical physics [8–10]. Aggregation also plays a central role in the theory of percolation [11], fractal formation [12], and network growth [13, 14].

Often, aggregation is driven by a constant injection of mass and consequently, the total mass grows indefinitely with time [15–20]. This is the case in chemical kinetics, and in particular polymerization where the aggregation rate depends on the number of clusters. Here, due to aggregation, the total number of clusters typically decreases with time or saturates at a finite value. In such aggregation processes, the system may undergo gelation: a giant cluster develops and eventually, it contains all of the mass in the system [21–23].

In this study, we are interested in complementary aggregation processes that describe the growth of random structures such as random trees and random graphs, relevant in computer and information science [24–27]. For example, in the Internet, clusters are autonomous systems; injection models the creation of new autonomous systems and aggregation describes merger of different autonomous systems [28]. Such random structures are typically grown by the following simple process: in each step nodes may be added with some probability and otherwise, clusters are merged. Consequently, both the number of nodes and the number of clusters grow with time.

We investigate aggregation processes with mass injection where the total merger rate does not depend on the total number of clusters. These are fundamentally different than aggregation processes underlying cloud formation and dust agglomeration where the total merger rate

depends on the number of clusters. Our main finding is that in such situations there is condensation rather than gelation. The system develops condensates that contain a finite fraction of the mass. These macroscopic condensates co-exist with microscopic clusters that contain the rest of the mass in the system.

In our formulation, mass is injected at a constant rate and clusters merge at a constant total rate. We address the three classic kernels $K_{i,j}$ for aggregation between clusters of size i and j , respectively: the constant rate $K_{i,j} = \text{const}$, the sum rate $K_{i,j} = i + j$, and the product rate $K_{i,j} = i \times j$ [2]. Each of these cases represents an elementary growing random structure. Generally, random structures such as random trees and random graphs are made of nodes interconnected by links. Mass injection represents addition of isolated nodes, and merger represents addition of a link between two nodes [25, 27]. In the constant rate process, two structures are picked at random and an added link connects the two. In the product rate process, two nodes, picked at random, are connected by an added link. Finally, the sum rate is a hybrid of the constant and the product cases: the link connects a randomly selected node and a randomly selected structure. We note that the constant aggregation rate models an ensemble of random growing trees (no cycles are formed), while the sum and the product rates model an ensemble of random growing graphs.

For the constant aggregation rate, the cluster size distribution decays exponentially with the cluster size. For both the sum and the product rates, where the aggregation rate grows with the aggregate size, the system undergoes a phase transition as a function of the injection rate. When the injection rate is smaller than some critical value, the system is in a condensate phase. A finite fraction of the total mass constitutes a macroscopic condensate, but the remaining fraction of mass is in the form of microscopic clusters. The condensate and the finite clusters coexist. When the injection rate is larger

than the critical rate, there are only finite clusters.

In the cluster phase, the distribution of cluster size generally decays as a power-law with the cluster size. However, different behaviors emerge in the condensate phase. For the product rate, the size distribution falls-off exponentially at large size. For the sum rate, however, the behavior is always power-law. Interestingly, in the latter case, the decay exponent is not monotonic. It decreases monotonically with the injection rate in the condensate phase but increases monotonically in the cluster phase.

The rest of this paper is organized as follows. We introduce the model, describe some of its basic features, and formulate the master equation approach in Sec. II. The constant rate, the sum rate, and the product rate are analyzed in sections III, IV, V, respectively. Generally, our focus is the size of the condensate and the tail of the cluster size distribution. We conclude in Sec. VI. Technical derivations of two results in sections IV and V are presented in appendices A and B.

II. THE MODEL

In our model, there are two independent and competing processes: mass injection and merger of clusters. In the first process, monodisperse elemental clusters are added to the system. This injection process occurs at a constant rate. In the second process, two clusters are merged. The mass of the resulting cluster is equal to the sum of the two original masses. The total merger rate is constant as well, and since both processes occur with constant rates, we may set one of them to unity without loss of generality. We therefore set the mass injection rate to r and the merger rate to one. Also, since the injection is monodisperse, we set this injection size as the mass unit. Initially, the system contains no clusters.

The total mass and the total number of clusters follow directly from these definitions. Each injection event increases the number of clusters by one and similarly, each merger event decreases the number of clusters by one. Thus, the average total number of clusters, $N(t)$, satisfies $dN/dt = r - 1$ and consequently, there is simple linear growth

$$N(t) = (r - 1)t. \quad (1)$$

We restrict our attention to situations where the number of clusters grows with time, $r > 1$.

Merger events conserve the total mass, and hence, the mass changes only through injection events. With each injection event, unit-size mass is added to the system, and thus, the average total mass, $M(t)$, obeys $dM/dt = r$. Consequently, the total mass also grows linearly with time,

$$M(t) = rt. \quad (2)$$

We investigate the cluster size distribution. Let $C_k(t)$ be the average number of clusters of size k at time t . This

quantity satisfies the master equation

$$\frac{dC_k}{dt} = r\delta_{k,1} + \frac{1}{2} \sum_{i+j=k} K_{i,j} C_i C_j - \sum_i K_{i,k} C_i C_k. \quad (3)$$

The initial condition is $C_k(0) = 0$. The first term accounts for mass injection and the last two terms account for merger. The kernel $K_{i,j}$ is defined as the aggregation rate between two clusters with size i and j . Since the process by which particles are selected is completely random, this equation is exact in the thermodynamic limit of an infinite number of particles or equivalently, the long time limit. The total merger rate is constant, thereby implying the following constraint on the aggregation rate

$$1 = \frac{1}{2} \sum_{i,j} K_{i,j} C_i C_j. \quad (4)$$

The total number of clusters is of course $N(t) = \sum_k C_k(t)$. Summing the master equation (3), and using the constraint (4), we confirm the linear growth of the total number of clusters (1). Similarly, the total mass is $M(t) = \sum_k k C_k(t)$. Only the first term in the master equation affects the evolution of the total mass, and summing the rate equations, we recover (2).

III. CONSTANT AGGREGATION RATE

For the constant aggregation rate, all pairs of clusters merge at the same rate, irrespective of their size. This is the simplest and the most widely used aggregation process with examples including fractal aggregates [29], domain growth [30], and random trees [31, 32]. We consider the following size-independent aggregation rate

$$K_{i,j} = \frac{2}{N^2}. \quad (5)$$

This constant satisfies the normalization (4). It decreases as the number of clusters increases so that the overall merger rate does not change with time.

Substituting this constant rate into the master equation (3), the cluster size density satisfies

$$\frac{dC_k}{dt} = r\delta_{k,1} + \frac{1}{N^2} \sum_{i+j=k} C_i C_j - \frac{2}{N} C_k. \quad (6)$$

The linear growth of the total number of clusters (1) and the total mass (2) suggest that the cluster size distribution also grows linearly with time. Indeed, the density of the smallest clusters obeys $dC_1/dt = r - 2C_1/N$ so that this quantity, too, grows linearly with time, $C_1(t) = N(t) \frac{r}{r+1}$. Thus, we write the cluster size density as a product of the overall density $N(t)$ and the time-independent cluster size distribution c_k ,

$$C_k(t) = N(t) c_k. \quad (7)$$

The cluster size distribution is normalized, $\sum_k c_k = 1$. This form is consistent with the initial condition, and it satisfies (6) when the cluster size distribution obeys the recursion equation

$$(1+r)c_k = r\delta_{k,1} + \sum_{i+j=k} c_i c_j. \quad (8)$$

We utilize the generating function technique [33] to solve this equation. Let $f(z)$ be the generating function

$$f(z) = \sum_{k=1}^{\infty} c_k z^k. \quad (9)$$

Normalization implies $f(1) = 1$. Multiplying Eq. (8) by z^k and summing over k , the generating function satisfies the quadratic equation $f^2(z) - (1+r)f(z) + rz = 0$. The solution is therefore

$$f(z) = \frac{r+1}{2} \left[1 - \sqrt{1 - \frac{4r}{(1+r)^2} z} \right]. \quad (10)$$

We can confirm that $f(z) = \frac{r}{1+r}z + \dots$, in agreement with the above expression for C_1 . Writing the generating function as a power-series, the cluster size distribution is obtained explicitly,

$$c_k = \frac{1+r}{4\sqrt{\pi}} \frac{\Gamma(k-1/2)}{\Gamma(k+1)} \left[\frac{4r}{(1+r)^2} \right]^k \quad (11)$$

where $\Gamma(x)$ is the Gamma function. Using the asymptotic property $\Gamma(x+r)/\Gamma(x) \simeq x^r$ as $x \rightarrow \infty$, we find

$$c_k \simeq \alpha k^{-3/2} \beta^k \quad (12)$$

with the constants $\alpha = \frac{1+r}{4\sqrt{\pi}}$ and $\beta = \frac{4r}{(1+r)^2}$. Therefore, the cluster size distribution decays exponentially, but there is an algebraic correction. As the injection rate approaches the merger rate, $r \rightarrow 1$, the cluster size distribution becomes algebraic $c_k \sim k^{-3/2}$. This limiting case coincides with the well-known behavior for time-independent constant aggregation rates [17].

We comment that the rate equation approach is exact only in the limit of an infinite number of particles. At any given time t , the number of clusters is finite and proportional to t , while fluctuations in the number of clusters are of the order of \sqrt{t} . The relative fluctuations in the cluster size distribution grow with cluster size and they provide a more stringent test of the applicability of the rate equation approach. When $C_k \sim 1$, fluctuations begin to dominate. From this criterion and Eq. (12) we see that the prediction (11) is valid up to a cutoff size that grows logarithmically with the total mass. Nevertheless for any fixed size, the prediction (11) becomes exact in the limit $t \rightarrow \infty$.

IV. SUM AGGREGATION RATE

Aggregation rates proportional to the sum of the cluster sizes are relevant in polymerization [34], coagulation

under shear-flows [5], and random graphs [25]. Subject to the constraint (4), the sum aggregation rate is

$$K_{i,j} = \frac{i+j}{NM}. \quad (13)$$

In this case, the master equation (3) becomes

$$\frac{dC_k}{dt} = r\delta_{k,1} + \frac{k}{2NM} \sum_{i+j=k} C_i C_j - \frac{kN+M}{NM} C_k. \quad (14)$$

We again seek a solution of the form (7). The cluster size distribution remains normalized, $\sum_k c_k = 1$, and it obeys the following recursion relation

$$(k+R)c_k = R\delta_{k,1} + \frac{k}{2} \sum_{i+j=k} c_i c_j \quad (15)$$

with the constant

$$R = \frac{r^2}{r-1}. \quad (16)$$

This recursion relation can be manually solved to find $c_1 = \frac{R}{R+1}$, $c_2 = \frac{1}{R+2} \left(\frac{R}{R+1} \right)^2$, etc. This procedure can be formally related to integer partitions following the solution procedure of Ref. [35]. Such a solution is useful only when the cluster size distribution decays sharply. Although it is difficult to obtain an explicit analytic solution as in (11), it is still possible to obtain many of the interesting properties of cluster size distribution from asymptotic analysis of the generating function.

The generating function (9) obeys the nonlinear ordinary differential equation

$$z(f-1) \frac{df}{dz} = R(f-z). \quad (17)$$

Derivatives of the generating function at $z = 1$ are related to the moments of the cluster size distribution. For example, the average cluster size follows from the first derivative, $\langle k \rangle = f'(1)$.

Differentiating (17) and then substituting $z = 1$ yields a quadratic equation for the average cluster size

$$R^{-1} \langle k \rangle^2 - \langle k \rangle + 1 = 0. \quad (18)$$

Naively, one expects that the average cluster size is the ratio between the total mass and the total number of clusters, $\langle k \rangle = \frac{M}{N} = \frac{r}{r-1}$. Indeed, this is a solution of (18). However, there is another solution $\langle k \rangle = r$. This solution is not physical when $r > 2$ since the product $N\langle k \rangle$ can not exceed the total mass in the system. Each solution is relevant in the appropriate range of the parameter r , so that the full solution is

$$\langle k \rangle = \begin{cases} r & 1 < r < 2 \\ \frac{r}{r-1} & 2 < r. \end{cases} \quad (19)$$

This assertion is supported by analysis below. The total mass contained by the clusters, $M_c = \sum_k kC_k$,

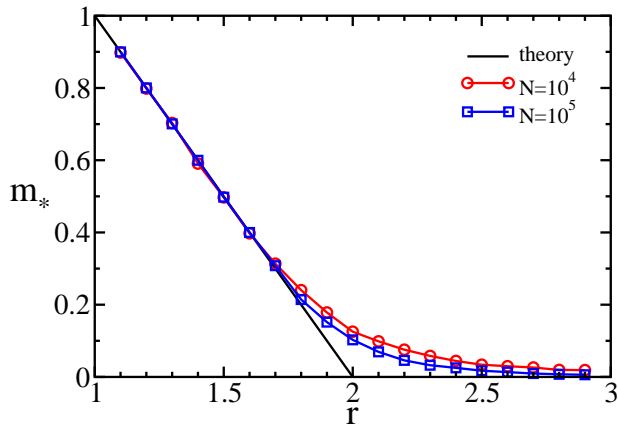


FIG. 1: The condensate mass m_* as a function of r for the sum rate. Shown in a solid line is the theoretical prediction (20). Shown in solid lines with symbols are Monte Carlo simulations results for the size of the largest cluster in the system.

is of course proportional to the average cluster size, $M_c = N \sum_k k c_k = N \langle k \rangle$. Therefore, finite clusters contain only a fraction of the mass when $r < 2$, but they contain all of the mass when $r > 2$.

This behavior can be reconciled with mass conservation only if there is a condensate of mass M_* that contains the remaining fraction $m_* = M_*/M$ of the mass in the system as follows (figure 1)

$$m_* = \begin{cases} 2 - r & 1 < r < 2 \\ 0 & 2 < r. \end{cases} \quad (20)$$

Thus the system undergoes a phase transition. When $1 < r < 2$, there is a condensate that contains a finite fraction of the mass. This condensate coexists with the finite clusters that contain the rest of the mass. The condensate contains nearly all of the mass in the limit $r \rightarrow 1$: when injection is very slow, the condensate “preys” on newly added mass. As the transition point is approached, the condensate mass vanishes, $m_* \rightarrow 0$ as $r \rightarrow 2$. When $r > 2$, the system contains only ordinary clusters.

The tail of the cluster size distribution can be evaluated from the $z \rightarrow 1$ behavior of the generating function. In general, $f(z)$ may contain both a regular component and a singular component, $f(z) = f_{\text{reg}}(z) + f_{\text{sing}}(z)$. The regular component is a power series in $(z - 1)$. Let us assume a singular behavior with the leading behavior $f_{\text{sing}} \propto (1 - z)^{\gamma-1}$ as $z \rightarrow 1$,

$$f(z) = \underbrace{1 + \langle k \rangle (z - 1) + \dots}_{f_{\text{reg}}(z)} + \underbrace{A(1 - z)^{\gamma-1} + \dots}_{f_{\text{sing}}(z)}. \quad (21)$$

In the limit $z \rightarrow 1$, this form satisfies the governing equation (17) when

$$\langle k \rangle \gamma = R. \quad (22)$$

The algebraic form of the generating function implies an algebraic form for the tail of the cluster size distribution,

$$c_k \sim k^{-\gamma}, \quad (23)$$

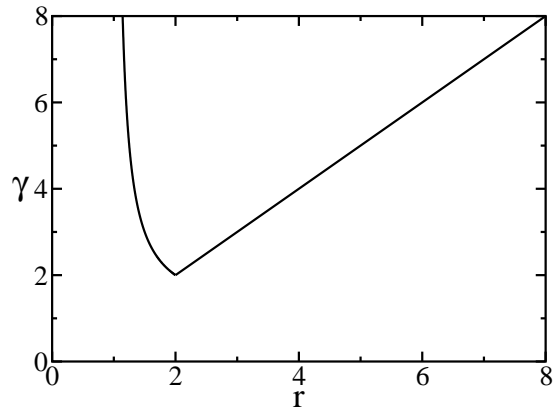


FIG. 2: The exponent γ versus r for the sum rate.

as $k \rightarrow \infty$. The exponent is found by substituting (19) into the relation (22). Therefore, there are two regimes of behavior

$$\gamma = \begin{cases} \frac{r}{r-1} & 1 < r < 2 \\ r & 2 < r. \end{cases} \quad (24)$$

We note two remarkable features. First, the cluster size density is algebraic both in the condensate phase and in the cluster phase. Second, the characteristic exponent is a non-monotonic function of the injection rate: it decreases monotonically with r in the condensate phase and it increases monotonically in the cluster phase (Fig. 2).

The exponent γ is minimal, $\gamma = 2$, at the phase transition point, $r = 2$. For $\gamma < 2$, mass conservation would be violated because the sum $\sum_k k c_k$ is divergent. The restriction $\gamma > 2$ justifies our previous choice of the non-trivial solution $\langle k \rangle = r$ in Eq. (19).

The behavior at the phase transition point requires a special treatment. We find that the cluster size density decays slightly faster than k^{-2} , namely

$$c_k \simeq \frac{2}{k^2 (\ln k)^2} \quad \text{as } k \rightarrow \infty. \quad (25)$$

The derivation of this result is detailed in Appendix A. With this logarithmic correction, the sum $\sum_k k c_k$ or the total mass in finite clusters, remain finite.

In ordinary gelation (or percolation), the cluster size distribution is algebraic *only* at the critical point; away from criticality, it has exponential tails. In the present case, the cluster size distribution exhibits a strikingly different behavior — it is algebraic everywhere while at the critical point there is a logarithmic correction.

The size of the condensate can be obtained directly by focusing on its dynamics. Let us assume that there is a giant cluster in the system with mass M_* . Its growth rate is $dM_*/dt = \sum_i K_{i,M_*} i$ and substituting the aggregation rate (13), we arrive at

$$\frac{dM_*}{dt} = \sum_i \frac{M_* + i}{NM} i \approx \frac{M_*(M - M_*)}{NM}. \quad (26)$$

In the second step, we made the approximation $M_* + i \approx M_*$ as the condensate is much larger than the rest of the clusters. When the condensate contains a finite fraction of the mass, $M_* = m_* M$, then from (26), we find $m_*(r-1) = m_*(1-m_*)$. Solving this equation, we recover the condensate mass (20).

This approach can also be used to derive the size of the largest cluster in the cluster phase. From (20), the quantity M_* is negligible compared with M , and therefore, the governing equation (26) reduces to $dM_*/dt \approx N^{-1}M_* \approx \frac{1}{(r-1)t}M$ so that

$$M_* \sim t^{\frac{1}{\gamma-1}}, \quad (27)$$

with $\gamma = r$ when $r > 2$. Therefore, the size of the largest cluster grows algebraically with time. This result can be alternatively derived using the algebraic behavior (23) and the extreme statistics criterion $1 \simeq N \sum_{k \geq M_*} c_k$.

We performed Monte Carlo simulations to test the theoretical prediction for the condensate mass (Fig. 1). In the simulations there are two elemental steps: injection with probability $r/(r+1)$ and aggregation with probability $1/(r+1)$. In an injection step, a cluster with unit mass is added into the system. In an aggregation step, two clusters, picked with probability proportional to the sum of the two masses, are merged. The simulations results represent an average over 100 independent runs for systems of size $M = 10^4$ and $M = 10^5$. We measured the size of the largest cluster in the system. Well below the transition point, there is excellent agreement between the theory and the simulations. The estimate (27) for the size of the largest cluster implies $M_*/M \sim M^{-(r-2)/(r-1)}$ when $r > 2$; similarly, $M_*/M \sim (\ln M)^{-1}$ at the transition point, $r = 2$. Therefore, the size of the largest cluster decays very slowly as a function of the system size near the transition point. Indeed, the simulation results slowly converge to the (thermodynamic) theoretical prediction in this regime.

V. PRODUCT AGGREGATION RATE

The product aggregation rate models polymerization and gelation [8, 9], as well as random graphs [24, 27], and in our case it has the following form

$$K_{i,j} = 2 \frac{i \times j}{M^2}. \quad (28)$$

The explicit rate equation for the product aggregation rate is

$$\frac{dC_k}{dt} = r \delta_{k,1} + \frac{1}{M^2} \sum_{i+j=k} i j C_i C_j - \frac{2}{M} k C_k. \quad (29)$$

Since the total mass appears in the denominator in the rate equation, we use a different normalization

$$C_k = M c_k. \quad (30)$$

The average number of clusters of size k still grows linearly with time. The transformation (30) reduces the master equation (29) to the nonlinear recursion equation

$$r c_k = r \delta_{k,1} + \sum_{i+j=k} i j c_i c_j - 2k c_k. \quad (31)$$

Given of the structure of this equation, it is convenient to use a different definition of the generating function

$$f(z) = \sum_{k=1}^{\infty} k c_k z^k. \quad (32)$$

The generating equation satisfies the very same equation (17) with

$$R = \frac{r}{2}. \quad (33)$$

Although the governing equation is the same, the boundary condition is different. Since the product aggregation rate grows with the cluster size, we expect that again there are two phases: a condensate phase and a cluster phase. The total mass contained in finite clusters is given by $M_c = M f(1)$. Therefore, in the condensate phase $f(1) < 1$ while in the cluster phase $f(1) = 1$. This change in the boundary condition results in a drastically different behavior.

We first discuss the cluster phase where $f(1) = 1$, and consequently, the analysis is a straightforward generalization of the above. The first derivative at $z = 1$ again satisfies $R^{-1}[f'(1)]^2 - f'(1) + 1 = 0$. At the critical point $R_c = 4$ and therefore $r_c = 8$. Solving this quadratic equation, the first derivative is

$$f'(1) = \frac{r}{4} \left(1 - \sqrt{1 - \frac{8}{r}} \right). \quad (34)$$

The first derivative is now the ratio between the second and the first moments of the cluster size distribution, $f'(1) = \langle k^2 \rangle / \langle k \rangle$. The tail behavior follows from the singular component of the generating function as in (21)

$$f(z) = \underbrace{1 + f'(1)(z-1) + \dots}_{f_{\text{reg}}(z)} + \underbrace{B(1-z)^{\gamma-2} + \dots}_{f_{\text{sing}}(z)}. \quad (35)$$

This again implies the power-law decay (23) for the cluster size distribution. We note that the unit shift in the exponent is due to the different definition of the generating function (32). From the governing equation (17), the exponent γ satisfies $(\gamma-1)f'(1) = R$, and the decay exponent is

$$\gamma = 1 + \frac{2}{1 - \sqrt{1 - \frac{8}{r}}}. \quad (36)$$

Similar to (24), the characteristic exponent grows linearly with the injection rate, $\gamma \simeq \frac{r}{2}$, at large injection rates (Figure 3). The minimum value, $\gamma = 3$, is achieved at

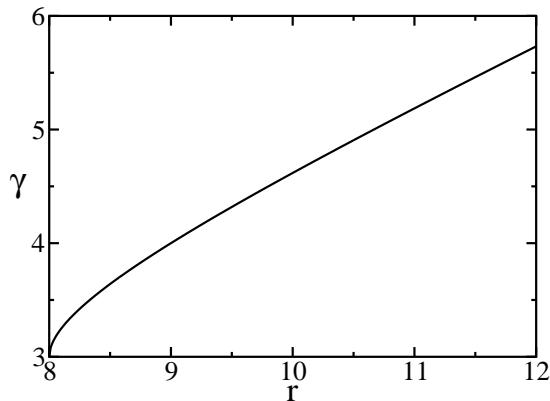


FIG. 3: The exponent γ versus r for the product rate.

the phase transition point. A more careful analysis is again required at the phase transition point; we find (the analysis is essentially the same as in the case of the sum rate, Appendix A) that $c_k \sim k^{-3}(\ln k)^{-2}$ as $k \rightarrow \infty$.

In the condensate phase, we are able to obtain the mass of the condensate only in the vicinity of the phase transition,

$$m_* \sim \exp \left[-\frac{\pi\sqrt{8}}{\sqrt{r-8}} \right], \quad (37)$$

as $r \downarrow 8$. The derivation of this result resembles that of Refs. [36, 37]; it is detailed in Appendix B. In contrast with the sum rate, the phase transition is now very gentle: all derivatives of the condensate mass vanish at the transition point $r = r_c$ [38, 39]. In practice, it may be difficult to locate the phase transition point (Figure 4). We comment that similar behavior was recently found in several models of growing networks [36, 37, 40–44].

As a signature of the phase transition, the quantity $f'(1)$ has a discontinuity at the phase transition point. In the condensate phase, this quantity is obtained, using the fact that $f(1) < 1$, directly from the governing equation (17), $f'(1) = R = r/2$. In the cluster phase it is given by (34). Therefore, the ratio between the second and the first moments has a jump at $r_c = 8$,

$$\frac{\langle k^2 \rangle}{\langle k \rangle} \rightarrow \begin{cases} 4 & r \uparrow r_c, \\ 2 & r \downarrow r_c. \end{cases} \quad (38)$$

A similar jump occurs in the Berezinskii-Kosterlitz-Thouless phase transition [38, 39].

Finally, we study the tail of the cluster size distribution. For this purpose, it is convenient to make the transformation $z = e^w$ so that the generating function (32) is redefined

$$f(w) = \sum_{k=1}^{\infty} k c_k e^{kw}. \quad (39)$$

Substituting this definition into the recursion equation

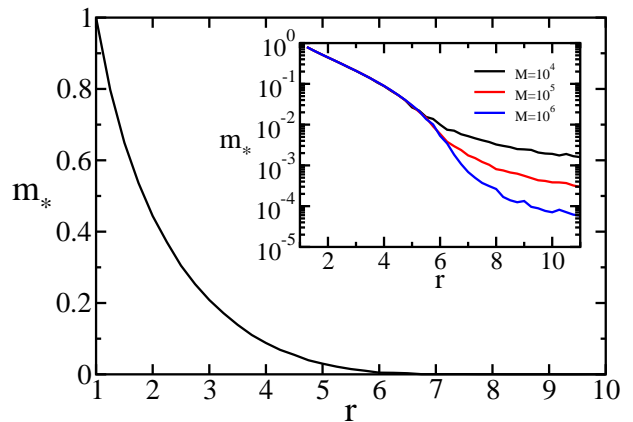


FIG. 4: The condensate mass m_* as a function of r obtained from Monte Carlo simulations of the aggregation process (product rate). The results are from a single run with $M = 10^6$ particles. The inset displays the same behavior using a semi-log scale. These simulation results represent an average over 100 independent realizations with a varying number of particles.

(31), the generating function obeys

$$\frac{df}{dw} = R \frac{f - e^w}{f - 1}. \quad (40)$$

The denominator suggests that $f(w)$ has a singularity at w_0 with $f(w_0) = 1$. From the definition (39), this implies the exponential decay $c_k \sim \exp(-k/k_0)$ with $k_0 = 1/w_0$. Since we can not solve for the generating function, we can not locate this singularity explicitly. Nevertheless, one can still deduce the behavior near this singularity using asymptotic analysis. Again, we assume that the generating function has a regular component and a singular component near $w = w_0$,

$$f(w) = \underbrace{1 + \dots}_{f_{\text{reg}}(w)} + \underbrace{A(w_0 - w)^{\nu-2} + \dots}_{f_{\text{sing}}(w)}. \quad (41)$$

Substituting this form into (40), and equating powers of $(w_0 - w)$ on both sides of the equation we obtain $\nu = 5/2$. Using the definition (39), the leading behavior of the singular component $1 - f(w_0) \sim (w_0 - w)^{\nu-2}$ implies an algebraic correction to the leading exponential decay, $c_k \sim k^{-\nu} \exp(-k/k_0)$ as $k \rightarrow \infty$. We conclude that the tail of the cluster size distribution decays as follows

$$c_k \sim k^{-5/2} e^{-k/k_0}. \quad (42)$$

The characteristic size can be related to the condensate mass in the vicinity of the phase transition as the characteristic size is expected to diverge in this limit, $k_0 \rightarrow \infty$. Consequently, the singularity is located close to the origin, $w_0 \rightarrow 0$. Let us estimate the behavior of the generating function near the origin. From the definition (39), we have $f(w=0) = 1 - m_*$. Also, from the governing equation we have $f'(0) = 4$ in the limit $r \uparrow 8$

as in (38). Therefore, $f(w) = 1 - m_* + 4w$ as $w \rightarrow 0$ and from the condition $f(w_0) = 1$, the location of the singularity is $w_0 = m_*/4$. Therefore, the characteristic size grows as follows

$$k_0 \sim 1/m_* \quad (43)$$

in the vicinity of the phase transition point, $r \uparrow 8$.

The tail behavior coincides with the critical behavior at sufficiently small sizes, $c_k \sim k^{-3}$ for $k \ll k_0$, and exponential decay, $c_k \sim \exp(-k/k_0)$, occurs beyond that scale, $k \gg k_0$. The two behaviors should of course match at $k \approx k_0$: this implies the proportionality constant in (42), $c_k \sim k_0^{-1/2} k^{-5/2} \exp(-k/k_0)$.

VI. CONCLUSIONS

In conclusion, we studied aggregation with constant injection of mass. In this process, the total number of clusters grows with time. For aggregation rates growing as the sum or the product of the cluster sizes, there are two phases: a condensate phase and a cluster phase. In the condensate phase, a condensate containing a finite fraction of the mass coexists with finite clusters, while in the cluster phase there are only finite clusters.

For the sum rate, the mass of the condensate is a linear function of the injection rate. Also, the cluster size distribution decays algebraically in both phases and interestingly, the decay exponent is a non-monotonic function of the injection rate. For the product rate the condensate mass is extremely small in the vicinity of the phase

transition point and consequently, the phase transition is very gentle. In this case, the tail of the cluster size distribution is exponential in the condensate phase but algebraic in the cluster phase.

We comment that there are two frameworks for describing aggregation processes: the Flory approach that allows interaction between giant and finite clusters [8] and the Stockmayer approach that allows for interactions between finite clusters only [9]. We used the more challenging former approach as it is the appropriate approach for modeling growing random structures [45].

The various aggregation processes correspond to different random growing structures, but our study focused only on the size of these structures. We note that this theoretical framework can be generalized to also study structural properties such as paths and cycles [27].

There are a number of possible extensions of this work. We focused on the three classic aggregation rates where the generating function obeys closed equations. This framework does not allow derivation of the necessary conditions for the emergence of a condensate as a function of the aggregation rate. Based on the sensitive algebraic behavior in both of the phases, we speculate that the sum rate may be the marginal case for condensation.

Acknowledgments. We thank the Isaac Newton Institute for Mathematical Sciences (Cambridge, England) and the Max Planck Institute for Physics of Complex Systems (Dresden, Germany), where this research was largely performed, for their hospitality. We acknowledge financial support from DOE grant DE-AC52-06NA25396 and NSF grant CHE-0532969.

-
- [1] M. von Smoluchowski, *Z. Phys.* **17**, 557 (1916).
 - [2] F. Leyvraz, *Phys. Rep.* **383**, 95 (2003).
 - [3] S. Chandrasekhar, *Rev. Mod. Phys.* **15**, 1 (1943).
 - [4] H. Pruppacher and J. Klett, *Microphysics of Clouds and Precipitations* (Kluwer, Dordrecht, 1998).
 - [5] R. L. Drake, in *Topics of Current Aerosol Research*, edited by G. M. Hidy and J. R. Brock (Pergamon, New York, 1972).
 - [6] S. K. Frieland, *Smoke, Dust and Haze: Fundamentals of Aerosol Behavior* (Wiley, New York, 1977).
 - [7] J. H. Seinfeld, *Atmospheric Chemistry and Physics of Air Pollution* (Wiley, Boston, 1986).
 - [8] P. J. Flory, *J. Amer. Chem. Soc.* **63**, 3083 (1941).
 - [9] W. H. Stockmayer, *J. Chem. Phys.* **11**, 45 (1943).
 - [10] P. J. Flory, *Principles of Polymer Chemistry* (Cornell University Press, Ithaca, 1953).
 - [11] D. Stauffer and A. Aharony, *Introduction to Percolation Theory* (Taylor & Francis, London, 1992).
 - [12] T. A. Witten and L. M. Sander, *Phys. Rev. Lett.* **47**, 1400 (1981).
 - [13] R. Albert and B. A. Barabasi, *Rev. Mod. Phys.* **74**, 47 (2002).
 - [14] S. N. Dorogovtsev and J. F. F. Mendes, *Adv. in Phys.* **51**, 1079 (2002).
 - [15] G. B. Field and W. C. Saslaw, *Astrophys. J.* **142**, 568 (1965)
 - [16] W. H. White, *J. Colloid Interface Sci.* **87**, 204 (1982).
 - [17] J. G. Crump and J. H. Seinfeld, *J. Colloid Interface Sci.* **90**, 469 (1982).
 - [18] E. M. Hendriks and M. H. Ernst, *J. Colloid Interface Sci.* **97**, 196 (1984).
 - [19] D. Aldous and B. Pittel, *Random Struct. Alg.* **17**, 79 (2000).
 - [20] Z. Cheng, S. Redner, and F. Leyvraz, *Phys. Rev. Lett.* **62**, 2321 (1989).
 - [21] R. M. Ziff, E. M. Hendriks, and M. H. Ernst, *Phys. Rev. Lett.* **49**, 593 (1982).
 - [22] P. G. J. van Dongen, *J. Phys. A* **20**, 1889 (1987).
 - [23] A. A. Lushnikov, *Phys. Rev. Lett.* **93**, 198302 (2004).
 - [24] B. Ballobás, *Random Graphs* (Academic Press, London, 1985).
 - [25] D. J. Aldous, *Bernoulli* **5**, 3 (1999).
 - [26] S. Janson, T. Luczak, and A. Rucinski, *Random Graphs* (John Wiley & Sons, New York, 2000).
 - [27] E. Ben-Naim and P. L. Krapivsky, *Phys. Rev. E* **71**, 026129 (2005).
 - [28] M. Fayed, P. L. Krapivsky, J. Byers, M. Crovella, S. Redner, and D. Finkel, *Computer Commun. Rev.* **33:2**, 41

(2003).

- [29] P. Meakin, *Fractals, Scaling and Growth Far From Equilibrium* (Cambridge University Press, New York 1998).
- [30] A. J. Bray, *Adv. Phys.* **43**, 357 (1994).
- [31] H. M. Mahmoud, *Evolution of Random Search Trees* (John Wiley, New York, 1992).
- [32] E. Ben-Naim, P. L. Krapivsky, and S. M. Majumdar, *Phys. Rev. E* **64**, 035101 (2001).
- [33] R. L. Graham, D. E. Knuth, and O. Patashnik, *Concrete Mathematics: A Foundation for Computer Science* (Reading, Mass.: Addison-Wesley, 1989).
- [34] R. M. Ziff, *J. Stat. Phys.* **23**, 241 (1980).
- [35] E. Ben-Naim and P. L. Krapivsky, *Phys. Rev. E* **73**, 03119 (2006).
- [36] P. L. Krapivsky and B. Derrida, *Physica A* **340**, 714 (2004).
- [37] S. N. Dorogovtsev, J. F. F. Mendes, and A. N. Samukhin, *Phys. Rev. E* **64**, 066110 (2001).
- [38] V. L. Berezinskii, *Sov. Phys. JETP* **32**, 493 (1970).
- [39] J. M. Kosterlitz and D. J. Thouless, *J. Phys. C* **6**, 1181 (1973).
- [40] D. S. Callaway, J. E. Hopcroft, J. M. Kleinberg, M. E. J. Newman, and S. H. Strogatz, *Phys. Rev. E* **64**, 041902 (2001).
- [41] P. L. Krapivsky and S. Redner, *Computer Networks* **39**, 261 (2002).
- [42] J. Kim, P. L. Krapivsky, B. Kahng, and S. Redner, *Phys. Rev. E* **66**, 055102 (2002).
- [43] M. Bauer and D. Bernard, *J. Stat. Phys.* **111**, 703 (2003).
- [44] C. Coulomb and M. Bauer, *Eur. Phys. J. B.* **35**, 377 (2003).
- [45] E. Ben-Naim and P. L. Krapivsky, *J. Phys. Cond. Mat.* **17**, S4249 (2005).

APPENDIX A: DERIVATION OF (25)

At the phase transition point $r = 2$ we have $\gamma = 2$ and therefore the leading singular term $f_{\text{sing}} \propto (1-z)^{\gamma-1}$ becomes regular. This suggests to use instead $f_{\text{sing}} \propto (1-z)u(z)$ where $u(z)$ vanishes slower than any power of $(1-z)$ as $z \rightarrow 1$. Thus at the phase transition point we employ the following expansion

$$f(z) = 1 + 2(z-1) + (z-1)u(z) + \dots \quad (\text{A1})$$

Substituting (A1) into (17) yields the differential equation

$$(z-1) \frac{du}{dz} + \frac{u^2}{2+u} = 0 \quad (\text{A2})$$

whose (implicit) solution is

$$-\frac{2}{u} + \ln u + \ln(1-z) = \text{const.} \quad (\text{A3})$$

In the limit $z \rightarrow 1$, the integration constant is negligible compared with the logarithmic term and consequently, $u \rightarrow 2/\ln(1-z)$. Indeed, u vanishes slower than any power of $(1-z)$ as $z \rightarrow 1$. Thus

$$f(z) = 1 + 2(z-1) + \frac{2(z-1)}{\ln(1-z)} + \dots \quad (\text{A4})$$

Inverting this expansion leads to Eq. (25) [36].

APPENDIX B: DERIVATION OF (37)

The mass of the condensate follows from the behavior of the generating function at $z = 1$, $m_* = 1 - f(1)$. To analyze the behavior near this region, we make the transformations

$$f(z) = 1 + xg(x), \quad (\text{B1a})$$

$$z = 1 - x. \quad (\text{B1b})$$

With these transformations, the equation for the generating function (17) is transformed into the following first-order nonlinear differential equation

$$xgg' + g^2 + Rg + R = 0. \quad (\text{B2})$$

In writing this equation, we kept only the leading order terms. Writing $\frac{g}{g^2+Rg+R}dg + \frac{1}{x}dx=0$, and integrating, we have

$$\frac{1}{2} \ln(g^2 + Rg + R) + \ln x - \frac{R}{2a} \tan^{-1} \left(\frac{g + R/2}{a} \right) = \text{const}$$

where $a = \sqrt{R - R^2/4}$. The integration constant can be evaluated by taking the $x \rightarrow 0$ limit. Using $m_* = -\lim_{x \rightarrow 0} xg(x)$, the first two terms in the above equation approach $\ln m_*$ in the limit $x \rightarrow 0$. Using $\lim_{x \rightarrow 0} g(x) = -\infty$, the last term approaches $\frac{R\pi}{4a}$. Hence

$$\begin{aligned} \frac{1}{2} \ln(g^2 + Rg + R) + \ln x - \frac{R}{2a} \tan^{-1} \left(\frac{g + R/2}{a} \right) \\ = \ln m_* + \frac{\pi R}{4a}. \end{aligned} \quad (\text{B3})$$

Since we are interested in the behavior near the phase transition point, we take the limit $r \rightarrow 8$. In this limit, we can replace R by 4 and also, the quantity $g^2 + Rg + R$ by $(g+2)^2$. Additionally, we may replace $\tan^{-1} \frac{g+2}{a}$ by $\frac{\pi}{2} - \frac{a}{g+2}$. With these substitutions, Eq. (B3) becomes

$$\ln(-g-2) + \ln x + \frac{2}{g+2} = \ln m_* + \frac{2\pi}{a}. \quad (\text{B4})$$

Next, we evaluate the left-hand side precisely at the phase transition point, $r = 8$. The critical behavior is detailed in Appendix A. Substituting $g = -2 - u$ and $x = 1 - z$ into (A3), gives

$$\ln(-g-2) + \ln x + \frac{2}{g+2} = \text{const.} \quad (\text{B5})$$

Substituting this into (B4) we obtain the condensate mass in the vicinity of the phase transition (37).